

Research and optimization of screening strategy for calcium-activated chloride channel modulators guided by electrophysiological characteristics

Received: 25 June 2025

Accepted: 6 February 2026

Published online: 23 February 2026

Cite this article as: Wang Y., Zheng K., Yang L. *et al.* Research and optimization of screening strategy for calcium-activated chloride channel modulators guided by electrophysiological characteristics. *Sci Rep* (2026). <https://doi.org/10.1038/s41598-026-39762-3>

Yanyan Wang, Kai Zheng, Liu Yang, Liying Liu, Haojian Han, Shuang Chen, Zhanning Qu, Kai Qin, Wansheng Zhang & Feng Hao

We are providing an unedited version of this manuscript to give early access to its findings. Before final publication, the manuscript will undergo further editing. Please note there may be errors present which affect the content, and all legal disclaimers apply.

If this paper is publishing under a Transparent Peer Review model then Peer Review reports will publish with the final article.

Research and Optimization of Screening Strategy for Calcium-Activated Chloride Channel Modulators Guided by Electrophysiological Characteristics

Yanyan Wang^{1,+}, Kai Zheng^{2,+}, Liu Yang¹, Liying Liu¹, Haojian Han¹, Shuang Chen³, Zhanning Qu¹, Kai Qin^{4,*,+}, Wansheng Zhang^{5,*,+} and Feng Hao^{1,*,+}

¹ College of Laboratory Medicine, Jilin Medical University, Jilin 132000, China; wyy111207@sina.com (Y.W.); y158434@126.com (L.Y.); 2394989743@qq.com (L.L.); wei9552551187@163.com (H.H.); aning12160610@163.com (Z.Q.)

² School of Public Health, Jilin Medical University, Jilin 132000, China; carane@163.com

³ School of Pharmacy, Jilin Medical University, Jilin 132000, China; chenshuang310-310@163.com

⁴ Jilin Changyuan Pharmaceutical Corporation Ltd, Jilin 132000, China

⁵ Jilin Medical College Affiliated Hospital Urology Surgery, Jilin 132000, China

* Correspondence: qinkai@jemincare.com (K.Q.); 171911604@qq.com (W.Z.); haof863@nenu.edu.cn (F.H.)

+ These authors contributed equally to this work

Abstract

Background: Calcium-activated chloride channels (CaCCs) are essential for epithelial secretion, neuronal transmission, and smooth muscle function. Among the Anoctamin family, Anoctamin 1 (ANO1) and Anoctamin 2 (ANO2) are classical CaCCs proteins. ANO1 has been identified as a potential therapeutic target due to its involvement in diseases such as cancer and cystic fibrosis. However, current high-throughput screening (HTS) systems face limitations in achieving subtype-specific detection and optimizing screening strategies.

Methods: Stable HTS cell models expressing ANO1 or ANO2 were constructed via lentiviral transduction in Fischer mouse thyroid (FRT) cells. The models were validated using flow cytometry, Reverse Transcription Polymerase Chain Reaction (RT-PCR), and YFP-

H148Q/I152L-based iodide fluorescence quenching assays. Patch-clamp electrophysiology was employed to characterize ANO1 and ANO2 current properties. Although these electrophysiological features have been previously reported, their application in HTS workflows had not been systematically evaluated.

Results: ANO1 displayed notable current rundown under sustained stimulation with high Ca^{2+} or agonist concentrations, whereas ANO2 maintained stable currents under identical conditions. Based on these findings, an optimized screening strategy was developed, incorporating agonist concentration gradients and the timing of inhibitor application. This approach improved the specificity and reliability of modulator detection.

Conclusions: A robust and functionally validated cell-based HTS platform for CaCCs modulator discovery was established. By integrating the electrophysiological characteristics of ANO1 into the screening design, the optimized strategy enhances the accuracy of identifying selective ANO1 modulators. This work provides a methodological basis for future mechanism-driven screening of CaCCs-targeted compounds.

Keywords: CaCCs; ANO1; ANO2; Electrophysiological Characteristics; HTS; Screening Strategy

1. Introduction

In 2008, research teams led by Uhtaek Oh from South Korea, Lily Yeh Jan from the USA, and Luis J. V. Galiotta from Italy confirmed for the first time that transmembrane protein 16A (TMEM16A) is a true calcium-activated chloride channel (CaCCs). Therefore, Professor Uhtaek Oh named it ANO1, which stands for "anoctamin," indicating its role as an anion channel^[1-3]. The anoctamin family includes ten members from ANO1 to ANO10, among which ANO1 and ANO2 are typical CaCCs.

Members of the anoctamin family, due to their diverse physiological distributions, play varied roles in different physiological and pathological mechanisms. ANO1 is significantly involved in airway and intestinal epithelial cells, smooth muscle cells, intestinal pacemaker cells, sensory neurons, and bodily fluid secretion^[4-6], participating in various physiological and pathological processes such as cell proliferation, migration, and cancer progression^[7, 8]. Inhibiting its activity could help treat diseases such as asthma, hypertension, diarrhea, pain, and cancer. ANO2 plays a crucial role in olfactory neurons and hippocampal neurons^[9, 10]. ANO6 is essential for the Ca²⁺-dependent exposure of phosphatidylserine in platelets, and its deficiency is the pathological basis of the hereditary bleeding disorder Scott syndrome^[11]. Recent studies have shown that inhibiting ANO6 activity can alleviate symptoms induced by the SARS-CoV-2 spike protein^[12]. ANO7 is strongly expressed in normal prostate gland cells but less so in cancer cells, making it an important prognostic marker for poor prostate cancer outcomes^[13, 14].

Early screening of CaCCs modulators primarily relied on calcium-sensitive fluorescent dyes (Fura-2, Fluo-4) to monitor intracellular Ca^{2+} concentrations. However, these approaches were often affected by calcium signaling cascades, resulting in limited channel specificity. To enable more direct monitoring of channel function, a YFP-H148Q/I152L-based iodide quenching screening system was developed. This system detects fluorescence decreases induced by intracellular iodide influx following channel activation, allowing for highly sensitive and high-throughput activity readouts^[15, 16]. This strategy has been successfully applied to the screening of the ANO1 inhibitor Ani91^[16], and its principle is illustrated in Figure 1.

The same approach has also been used for the identification of modulators targeting other chloride channels, such as the volume-regulated anion channel (VRAC) ^[17]. Patch-clamp electrophysiology remains the gold standard for validating functional changes, particularly suitable for characterizing current kinetics. In parallel, virtual screening serves as a complementary approach during the molecular design phase, providing mechanistic predictions and assisting in the optimization of candidate compounds^[18-20].

Among the currently discovered regulators of CaCCs, there is a notable issue of insufficient specificity, particularly with inhibitors of ANO1 such as T16Ainh-A01, CaCCinh-A01, and Monna, which also inhibit ANO2 to varying degrees^[21]. While highly specific inhibitors like Ani9 demonstrate strong selectivity for ANO1, such highly specific

inhibitors constitute a very small proportion^[22]. Moreover, the discovery of ANO1 activators remains challenging. In the field of ANO1 activator research, no substances capable of directly activating ANO1 have been identified so far. Both Eact and Fact are indirect activators that influence ANO1 activity through distinct indirect mechanisms ^[23]. Given the current state of regulator development, this study raises a question: Why are there so few direct agonists for ANO1, and could this scarcity be due to the screening methods and strategies employed?

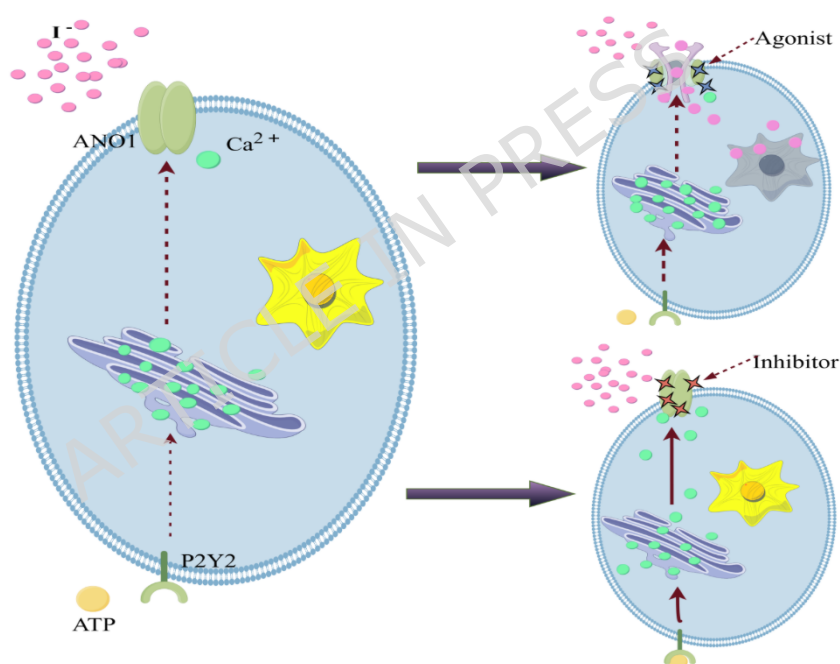


Figure 1: Schematic Diagram of Yellow Fluorescent Protein Iodide Ion Quenching Method (by Fig Draw). ANO1: Anoctamin1; Ca^{2+} : Calcium ion; YFP: Yellow fluorescent protein mutant YFP-H148Q/I152L; P2Y2: Adenosine triphosphate receptor P2Y2; ATP: Adenosine triphosphate

2. Materials and Methods

2.1. Materials

Fetal bovine serum (Clark, USA), F12 basal medium, 1640 basal medium, and trypsin (Gibco, USA) were used for cell culture. Lipofectamine 3000 transfection reagent and the BCA protein assay kit were purchased from Thermo Fisher (Shanghai, China). Plasmids including pcDNA3.1-ANO1-EGFP, pcDNA3.1-ANO2-EGFP, and pcDNA3.1-YFP-H148Q/I152L were previously stored in our laboratory. Eact, Niflumic acid (NFA, a Cl⁻ channel blocker), and Ionomycin were all obtained from Sigma-Aldrich (Shanghai, China). The RT-PCR kit was purchased from Takara Bio (Dalian, China), and the PCR kit, DNA marker, and agarose were purchased from TransGen Biotech (Beijing, China) and OXOID (Thermo Fisher Scientific, Shanghai, China), respectively. Antibiotics including puromycin and blasticidin were obtained from Solarbio (Beijing, China).

2.2. Cell Culture

The Fischer Rat Thyroid (FRT) cell line was kindly provided by Professor Tonghui Ma from Northeast Normal University (Jilin, China), while the Human Embryonic Kidney 293T (HEK293T) cell line was purchased from the Cell Bank of the Shanghai Institute of Biochemistry and Cell Biology. In our laboratory, the FRT cells are cultured in F12 medium supplemented with 10% fetal bovine serum, and the HEK293T cells are maintained in RPMI 1640 medium containing 10% fetal bovine serum.

2.3. Establishment of Stable Cell Lines Expressing ANO1-YFP and ANO2

To establish FRT cell lines stably expressing ANO1/ANO2 and the YFP mutant, 9×10^5 FRT cells were seeded per well in a 6-well plate. After cell attachment, various concentrations of puromycin (0–3.0 $\mu\text{g}/\text{mL}$) and blasticidin (0–60 $\mu\text{g}/\text{mL}$) were added. Each group included three replicates. After 4–6 days of selection, the antibiotic concentrations that resulted in approximately 90% cell death were identified and used as the optimal concentrations for subsequent stable selection.

Lentiviral packaging and transduction were performed as follows: 293T cells were co-transfected with lentiviral packaging plasmids (RRE, REV, and VSVG) and lentiviral vectors encoding the target genes (PLVX-Blasticidin-ANO1-EGFP, PLVX-Blasticidin-ANO2-EGFP, and PLVX-Puro-YFP-H148Q/I152L) using Lipofectamine 3000. The collected viral supernatants were used to infect FRT cells. The transduction was performed sequentially, first with ANO1-EGFP or ANO2-EGFP (which are membrane-localized proteins fused with EGFP for direct visualization), followed by cytoplasmic YFP-H148Q/I152L. After infection, cells were subjected to blasticidin or puromycin selection to obtain stable transductants, and monoclonal high-expression lines were established by limiting dilution.

To verify transduction efficiency, flow cytometry analysis (BD, USA) was performed to detect fluorescent protein expression.

Untransfected FRT cells were used as the negative control. Based on emission spectra, the FL2-A channel (585 ± 20 nm) was used to detect the EGFP signal from ANO1 or ANO2, and the FL1-A channel (530 ± 15 nm) was used to detect YFP-H148Q/I152L expression, enabling clear distinction between the two fluorescent tags.

2.4. RT-PCR Analysis to Verify Gene Expression of YFP, ANO1, and ANO2 in FRT Cells

Using a reverse transcription kit, cDNA is synthesized corresponding to the RNA extracted from FRT cells. Specific primers for the ANO1, ANO2, and YFP-H148Q/I152L genes were designed for this study (see Table 1). The cDNA serves as a template for PCR amplification. Following the amplification, the PCR products are subjected to agarose gel electrophoresis and visualized using a gel imaging system (BIO-RAD, USA). This allows for the assessment of the specificity and efficiency of the amplification, ensuring that the target genes are being correctly expressed in the cell lines.

Table 1. Primer sequence

Primer	Sequence(5'to3')	Base number
ANO1 forward primer	TTTCCGGATGGAGGAGTGTG	20
ANO1 reverse primer	TGTAGAGGTACACCAGGCGA	20
ANO2 forward primer	TACCGCATGGAAGAGTGTGC	20
ANO2 reverse primer	ACACAAGGCGGGGGATAAAG	20
YFP-H148Q/I152L forward primer	ATGTCCAAGGCGGAGGAG	18
YFP-H148Q/I152L reverse primer	TCACTTGTAGAGCTCGTCCA	20
	GTCGTGACAACGGCTCC	18
β -actin forward primer	AGGTCTCAAACATGATCTGGGT	20

2.5. Patch-Clamp Technique to Investigate the Electrophysiological Properties of ANO1 and ANO2

Patch-clamp electrophysiology, a classical method for real-time monitoring of ion channel activity, continues to play a key role in functional validation and mechanistic investigation. In this study, both whole-cell and inside-out patch-clamp configurations were employed to systematically analyze the electrophysiological properties of ANO1 and ANO2 from the perspectives of overall channel response and intracellular regulation.

The internal solution was prepared using an EGTA/Ca-EGTA-NMDG buffering system, with free Ca^{2+} concentrations (0, 600 nM, and 25 μM) set by adjusting the ratio of EGTA to Ca-EGTA. The solution contained 146 mM CsCl, 2 mM MgCl_2 , 8 mM HEPES, and 5 mM chelator, adjusted to pH 7.3 with a final osmolality of approximately 300 mOsm. Free Ca^{2+} concentrations were calculated using the MaxChelator software. The external perfusion solution consisted of 140 mM NaCl, 5 mM KCl, 2 mM MgCl_2 , 1 mM CaCl_2 , 10 mM HEPES, and 10 mM glucose, adjusted to pH 7.4 with a similar osmolality of ~ 300 mOsm. A Ca^{2+} -free control solution was also included. All solutions were sterilized by filtration through a 0.22 μm

membrane, and perfusion was maintained at a flow rate of 1–2 mL/min to allow rapid solution exchange.

Patch-clamp recordings were performed using an EPC10 amplifier (HEKA) and an eight-pole Bessel filter (Warner Instruments). The sampling rate was 10 kHz, with a low-pass filter set at 2 kHz. The resistance of the glass microelectrodes was maintained between 3 and 5 M Ω . Data acquisition and analysis were conducted using pClamp 10.0 software.

2.5.1. Whole-Cell Patch-Clamp Technique Methodology

The whole-cell configuration was used to record ion current responses across the entire membrane patch. FRT-ANO1-YFP and FRT-ANO2 cells were seeded on pretreated glass coverslips, and cells with well-defined morphology and clear fluorescence expression were selected for recording under an inverted fluorescence microscope. Step pulses from -100 mV to +100 mV were applied from a 0 mV holding potential, with each pulse lasting 800 ms, to evaluate the activation characteristics of the channels.

2.5.2. Inside-Out Patch-Clamp Technique Methodology

The inside-out configuration was used to investigate the mechanism by which intracellular Ca²⁺ directly regulates channel activity. After achieving a high-resistance seal, the micropipette was

rapidly withdrawn to form an inside-out patch with the intracellular side of the membrane exposed to the bath solution. Different free Ca^{2+} concentrations were applied via a rapid perfusion system to induce channel activation, and the resulting membrane currents were recorded. Data acquisition and recording parameters were identical to those used in the whole-cell configuration.

2.6. Fluorescence Kinetic Analysis for Evaluating ANO1 Functional Regulation

To quantitatively evaluate changes in ANO1 activity under different pharmacological conditions, a functional assay model was established using FRT cells stably expressing ANO1-YFP-H148Q/I152L. Cells were seeded into black-walled, clear-bottom 96-well plates and cultured for 48 hours until reaching approximately 90% confluence in each well. The experiment included three groups: an Ionomycin gradient group (final concentrations of 5, 10, and 20 μM), an ANO1 inhibitor group treated with NFA (500 μM), and a PBS control group. Each condition was tested in triplicate.

Prior to treatment, all wells were prewashed with PBS containing Ca^{2+} and Mg^{2+} to eliminate background ion interference, leaving 50 μL of residual buffer per well. To simulate elevated intracellular Ca^{2+} levels, cells in the Ionomycin group were incubated at room temperature for 2 minutes. The NFA group was incubated with the

inhibitor for 10 minutes to provide a negative regulatory condition. The control group received an equal volume of PBS.

Fluorescence measurements were performed using a CLARIO^{star} Plus multi-mode plate reader (BMG Labtech, Germany), with excitation at 500 nm and emission at 540 nm. The total acquisition time was 14 seconds, with a sampling frequency of 5 Hz. The first 2 seconds were used to establish a fluorescence baseline. Starting at the 2-second mark, 120 μ L of NaI-PBS buffer was injected into each well at a rate of 180 μ L/s using the instrument's automated injection system. Pump 1 was used for the Ionomycin and PBS groups, while Pump 2 was dedicated to the NFA group to avoid reagent cross-contamination.

After data acquisition, fluorescence quenching curves were exported to the MARS analysis software (integrated within the CLARIO^{star} system). The initial slope of the linear portion of the YFP signal decay was calculated as an indicator of channel activity, allowing for comparative analysis of ANO1 function under different pharmacological conditions.

2.7. Z'-Factor Assessment of ANO1 High-Throughput Screening Cell Model Stability

The Z' -factor (Z-prime factor) is an important statistical parameter used to evaluate the stability and reproducibility of HTS systems. A Z' -factor closer to 1 indicates a higher signal-to-noise

ratio and greater experimental reliability. Generally, a Z' -factor greater than 0.4 is considered indicative of a robust and stable screening system. In this study, the Z' -factor was calculated using the following formula: $Z' = 1 - 3 \times \frac{SD_{\text{positive}} + SD_{\text{BACK}}}{M_{\text{positive}} - M_{\text{BACK}}}$. To assess the stability of the ANO1-YFP-H148Q/I152L stably expressing cell model in the fluorescence quenching assay, cells were seeded into black-walled, clear-bottom 96-well plates and cultured for 24 hours prior to testing. Positive and negative controls were assigned by column: columns 1-6 served as the positive control group, with each well receiving 50 μL of 20 μM Ionomycin; columns 7-12 served as the negative control group, with each well receiving an equal volume of PBS. After three washes with PBS, 50 μL of buffer was retained in each well to establish the baseline background.

Fluorescence quenching kinetics were measured using a CLARIO^{star} Plus multi-mode plate reader (BMG Labtech, Germany), following the detection protocol described in Section 2.6. The resulting fluorescence intensity data were used to calculate the mean and standard deviation for each group, from which the Z' -factor was subsequently derived. This parameter provides a quantitative assessment of assay stability and serves as a quality control benchmark for subsequent high-throughput screening experiments.

2.8. Concentration- and Time-Dependent Activation of ANO1 by Eact

To systematically evaluate the regulatory effect of the ANO1 agonist Eact on channel function, a quantitative detection method based on the YFP-H148Q/I152L quenching system was established. Kinetic analyses were performed from both concentration–response and time–response perspectives.

2.8.1. Dose-response curve for Eact, an indirect activator of ANO1

FRT cells stably co-expressing ANO1 and YFP-H148Q/I152L were seeded into black-walled, clear-bottom 96-well plates and cultured until the cell confluence reached approximately 90% per well. The experiment included an Eact gradient group and a PBS control group, each tested in triplicate. Eact was applied at final concentrations of 1, 2.5, 5, 10, 20, 40, 60, 80, and 100 μM , while the control group received an equal volume of $\text{Ca}^{2+}/\text{Mg}^{2+}$ -containing PBS buffer. Cells were incubated at room temperature for 2 minutes prior to fluorescence quenching kinetics detection.

YFP fluorescence quenching was measured using a CLARIO^{star} Plus multi-mode plate reader (BMG Labtech, Germany) under the parameters described in Section 2.6. After data acquisition, fluorescence quenching curves were exported, and the initial quenching slope for each well was calculated using MARS software.

Dose-response curves plotting Eact concentration against the corresponding slope values were generated in GraphPad Prism 8 to establish the concentration-dependent activation profile of ANO1 and assess the agonistic potency of Eact at different concentrations.

2.8.2. Effect of Eact on the Sustained Activation of ANO1 Channels

Based on the dose-response analysis, further investigation was conducted to examine the effect of different Eact concentrations on the stability of channel opening. A high-concentration group (60, 80, 100, 120, 140, and 160 μM) and a low-concentration group (1, 2, 4, 6, 8, and 10 μM) were established. For each concentration, fluorescence quenching assays were performed at eight designated time points (0, 5, 10, 20, 30, 40, 50, and 60 minutes) to monitor the dynamic changes in channel activity over time.

As in previous analyses, the initial slope of the fluorescence quenching curve was used to represent channel activation. The slope values at different time points were compared between high and low Eact concentrations to characterize the kinetic patterns of channel activation. This allowed assessment of the dose-dependent persistence of ANO1 channel opening and provided further insights into the temporal dynamics of ANO1 regulation by Eact.

2.9. Optimization of Screening Strategy for ANO1 Modulator High Throughput Screening Model

Based on the electrophysiological characteristics of ANO1 derived from electrophysiological experiments, the screening strategy for ANO1 modulators using the YFP iodide quenching method is optimized.

2.9.1. Optimization of ANO1 Agonist Screening Strategy

Following the findings from experiment 4.8.2 regarding the maximum duration of ANO1 channel opening under high concentration agonist conditions, this duration is used as the maximum operational time for high throughput screening. The high throughput screening protocol is optimized by adjusting the concentrations of agonists to evaluate their impact on channel opening duration and to identify the most effective modulators.

2.9.2. Optimization of ANO1 Inhibitor Screening Strategy

In the high throughput screening of ANO1 inhibitors, the order of drug addition is optimized to enhance the specificity of inhibitors. The suitable concentration of agonist to be added first is determined by analyzing the effects of high and low concentrations of Eact on ANO1 channel opening time, ensuring the efficiency and sustainability of the high throughput screening process.

2.10. Statistical Analysis

Experimental data are statistically analyzed using SPSS version 25.0. Data are presented as mean \pm standard deviation (mean \pm SD). Comparisons between two groups are conducted using the t-test, while comparisons among multiple groups involve one-way ANOVA, with $P < 0.05$ considered statistically significant. Graphs of experimental data are created using GraphPad Prism 8, schematic diagrams of experimental principles are drawn using Science Slides, and bioinformatics analyses are conducted using MEGA11 software.

3. Results

3.1. Establishment and validation of a stable expression model for ANO1-YFP-H148Q/I152L and ANO2 in FRT cells.

By constructing a lentiviral expression vector containing the ANO1, ANO2, and YFP-H148Q/I152L genes (See supplementary materials figure S1), and employing lentiviral infection along with antibiotic selection, we successfully established FRT cell lines that stably express these proteins. Fluorescence microscopy (Olympus, Japan) and flow cytometry validation revealed that both ANO2 and ANO1-EGFP fusion proteins exhibited stable expression on the cell membrane, whereas YFP-H148Q/I152L primarily localized to the cytoplasm (Figure 2A). The transfection efficiency exceeded 96%, with ANO1-YFP-H148Q/I152L approaching 100% (Figure 2B). RT-PCR

results indicated that the specific bands for ANO1, ANO2, and YFP-H148Q/I152L matched the sizes of the amplified products from the designed primers (Figure 2C), confirming successful gene expression. These high-purity cell samples provide a solid foundation for subsequent functional assays and patch-clamp experiments.

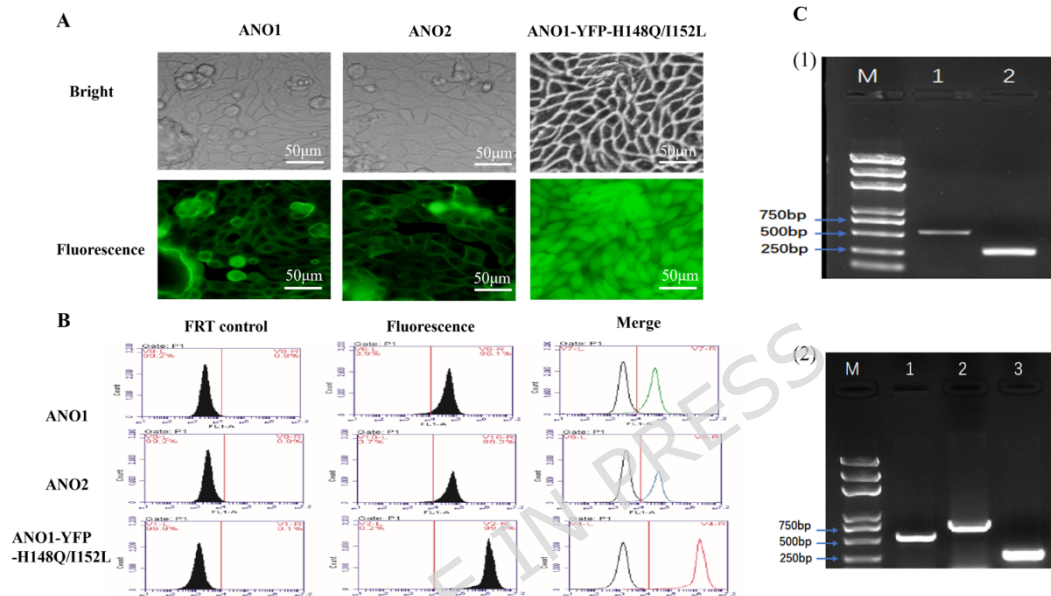


Figure 2: Establishment and validation of a stable expression model for ANO1-YFP-H148Q/I152L and ANO2 in FRT cells. A: Fluorescence images of FRT cells stably transfected with ANO2, ANO1, and ANO1-YFP-H148Q/I152L. Bright: bright-field image of the cells; Fluorescence: fluorescence image of the cells (40× magnification); B: Flow cytometry analysis of the purity of FRT cells stably transfected with ANO2, ANO1, and ANO1-YFP-H148Q/I152L; C: RT-PCR validation of gene expression of YFP-H148Q/I152L, ANO1, and ANO2 in FRT cells: (1) ANO2 stable transfectants; M: DNA marker; Lane 1: ANO2-specific band; Lane 2: β-actin; (2) ANO1-YFP-H148Q/I152L stable transfectants; M: DNA marker; Lane 1: ANO1-specific band; Lane 2:

YFP-H148Q/I152L-specific band; Lane 3: β -actin. The original gel, which includes the cropped regions, is shown in Supplementary Figure 2.

3.2. Patch-Clamp Technique to Investigate the Electrophysiological Properties of ANO1 and ANO2

3.2.1. Whole-Cell Patch-Clamp Technique Methodology

ANO1 and ANO2, as classic calcium-activated chloride channels (CaCCs), were evaluated for their calcium sensitivity and calcium-activated properties using the patch-clamp technique. In the whole-cell configuration, the concentration of calcium ions within the electrode solution was controlled to achieve varying degrees of activation of ANO1 and ANO2 channels, and current responses under different voltages were recorded. The findings include: 1. ANO1 and ANO2 can be activated by calcium ions, producing typical CaCCs currents. Under positive voltage stimulation, the increase in current is more pronounced with increasing clamp voltages, while under negative voltage stimulation, the increase in current is smaller. The I-V curve exhibits distinct outward rectifying characteristics.; 2. As the concentration of calcium ions increases, the activation currents of ANO1 and ANO2 also increase accordingly, as shown in Figures 3.; 3.

At a calcium ion concentration of 25 μ M, the use of the CaCCs inhibitor NFA significantly inhibits the whole-cell currents produced by ANO1 and ANO2. Notably, the whole-cell current produced by ANO2 at the same calcium concentration is significantly lower than that of ANO1, indicating that ANO2 is less sensitive to calcium ions than ANO1, as seen in Figure 3K. These results provide important foundational information for understanding the functions of ANO1 and ANO2 under physiological and pathological conditions, and contribute to further research and development of drugs targeting these channels.

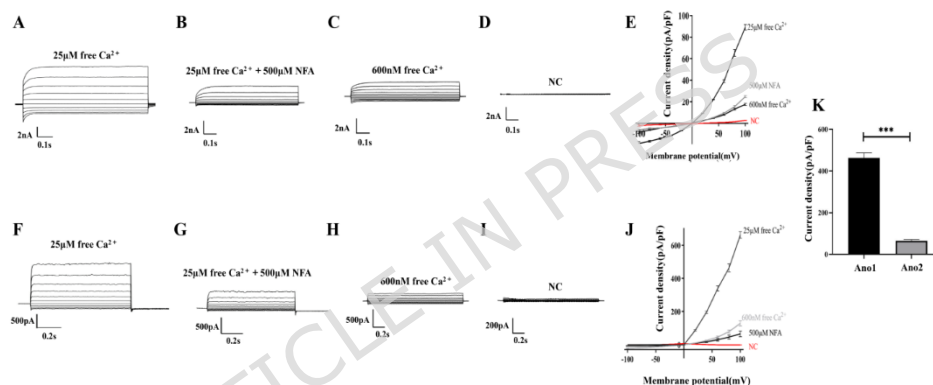


Figure 3: Whole-cell Patch-Clamp Analysis of ANO1 and ANO2 Functionality and Calcium Sensitivity. A: Whole-cell current

activated by 25 μ M calcium ions in ANO1; B: Inhibition of 25 μ M calcium ion-activated ANO1 current by the CaCCs inhibitor NFA; C: Whole-cell current activated by 600 nM calcium ions in ANO1; D: Negative control: Whole-cell current in untransfected empty FRT cells at 25 μ M calcium ion concentration; E: Current density-voltage (I-V) curves corresponding to panels A-D, where current density (pA/pF) = steady-state current / membrane capacitance; F: Whole-cell current activated by 25 μ M calcium ions in ANO2; G: Inhibition of 25 μ M

calcium ion-activated ANO2 current by the CaCCs inhibitor NFA; H: Whole-cell current activated by 600 nM calcium ions in ANO2; I: Negative control: Whole-cell current in untransfected empty FRT cells at 25 μM calcium ion concentration; J: Current density–voltage (I–V) curves corresponding to panels F–I, where current density (pA/pF) = steady-state current / membrane capacitance; K: Whole-cell current generated by 25 μM calcium ions activating ANO1 and ANO2 at +80 mV voltage (mean \pm SD, $n = 3$, $***P < 0.001$).

3.2.2. Whole-cell patch-clamp investigation of calcium concentration-dependent gating kinetics of ANO1 and ANO2 channels over time.

Whole-cell patch-clamp recordings were performed to evaluate the time-dependent current behavior of ANO1 and ANO2 channels under sustained intracellular calcium stimulation. As shown in Figure 4A, ANO1 exhibited typical CaCCs currents in response to 25 μM free Ca^{2+} . However, after 10 minutes of continuous activation, the current amplitude was markedly reduced, accompanied by a noticeable decrease in the I–V slope. This current attenuation (rundown) is consistent with previously reported findings^[1]. In contrast, under 600 nM Ca^{2+} stimulation, ANO1 currents remained relatively stable over the same period. Further comparison revealed that ANO2 exhibited no significant current rundown under either 25 μM or 600 nM Ca^{2+} conditions (Figure 4B), indicating greater current stability.

To quantitatively assess the stability differences between the two channels under different calcium concentrations, the percentage decrease in whole-cell current after 10 minutes of activation at +80 mV was calculated (Figure 4C). The results showed that ANO1 exhibited a significantly greater current decline than Ano2 under 25 μM Ca^{2+} ($P < 0.001$), whereas no significant rundown was observed for either channel under 600 nM Ca^{2+} .

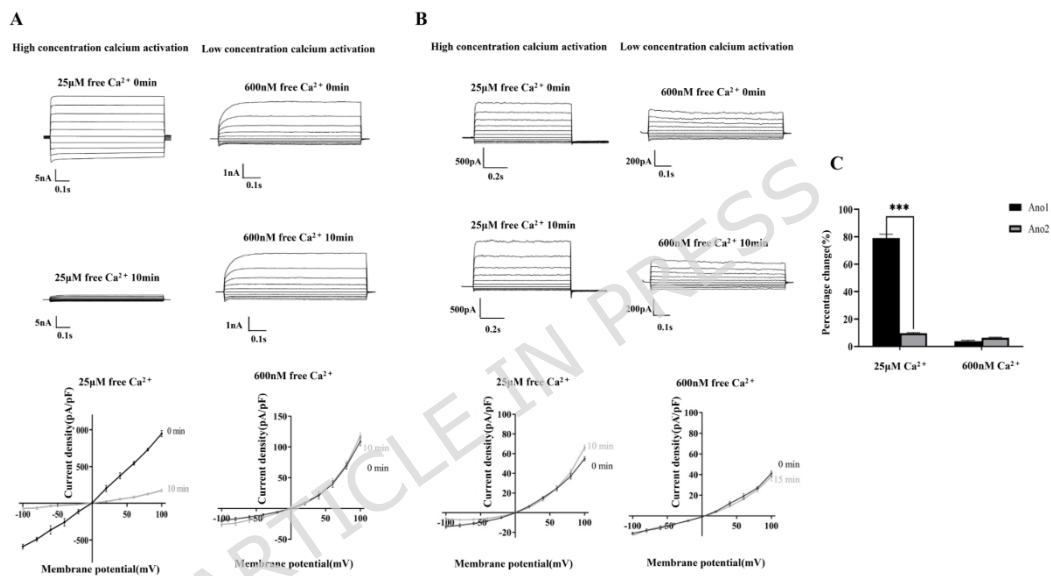


Figure 4: Investigation of the Time-Dependent Opening of ANO1 and ANO2 Channels under Sustained Activation by Different Calcium Ion Concentrations using Whole-Cell Patch-Clamp Technique. A: Time-dependent changes in whole-cell current activated by high and low concentrations of calcium ions for ANO1 opening; B: Time-dependent changes in whole-cell current activated by high and low concentrations of calcium ions for ANO2 opening; C: Percentage decrease in whole-cell current for ANO1 and ANO2 after

10 minutes of exposure to high and low concentrations of calcium ions at +80 mV (mean \pm SD, $n = 3$, $***P < 0.001$).

3.2.3. Inside-Out Patch-Clamp Technique Methodology

To further characterize the calcium responsiveness of Ano channels, inside-out patch-clamp recordings were performed. At a holding potential of -50 mV, exposure to 25 μ M Ca^{2+} robustly activated ANO1, eliciting a large Ca^{2+} -activated current. However, the current exhibited a progressive decline during sustained high-calcium stimulation, displaying a pronounced time-dependent rundown (Figure 5A). In contrast, under identical conditions, ANO2 generated a stable and long-lasting Ca^{2+} -activated current in response to 25 μ M Ca^{2+} , without any noticeable rundown throughout the recording period (Figure 5B).

These inside-out data align well with the observations obtained from whole-cell recordings and further demonstrate a clear difference between ANO1 and ANO2 in their ability to maintain current stability under high-calcium activation. This intrinsic divergence in channel stability suggests that dynamic current behavior may serve as a functional parameter for guiding the development of highly specific CaCCs modulators.

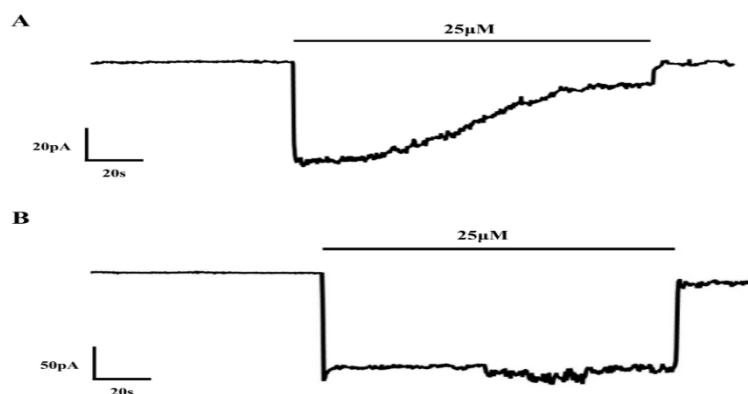


Figure 5: Electrophysiological characteristics of ANO1 [A] and ANO2 [B] recorded by the inside-out patch-clamp technique.

3.3. Functional Validation of the High-Throughput Screening Cell Model for ANO1 Modulators

To validate the functionality of the ANO1 high-throughput screening cell model, fluorescence-quenching kinetics assays were performed using the indirect ANO1 activator Ionomycin and the CaCCs inhibitor NFA. The results showed that in ANO1-expressing cells, the slope of the fluorescence-quenching curve increased in a concentration-dependent manner following Ionomycin treatment, with statistically significant differences compared with the negative control group ($P < 0.01$), as shown in Figures 6A and 6D.

To exclude background contributions from the parental cell line, parental FRT cells were examined under the same treatment conditions. The results demonstrated that FRT cells exhibited minimal fluorescence-quenching responses across all Ionomycin concentrations (Figure 6B), and the corresponding slope values

showed no significant differences (Figure 6E), indicating the absence of endogenous Ca^{2+} -activated conductance capable of generating a quenching signal. Thus, the functional readout in this assay originates predominantly from exogenously expressed ANO1.

Furthermore, NFA markedly suppressed the Ionomycin-induced activation of ANO1 (Figures 6C and 6F, $P < 0.001$), confirming that the model responds appropriately to both ANO1 activators and inhibitors.

Taken together, these findings demonstrate that the ANO1 cell model possesses high specificity, defined pharmacological sensitivity, and a favorable signal-to-noise ratio, supporting its suitability for high-throughput screening of ANO1 modulators.

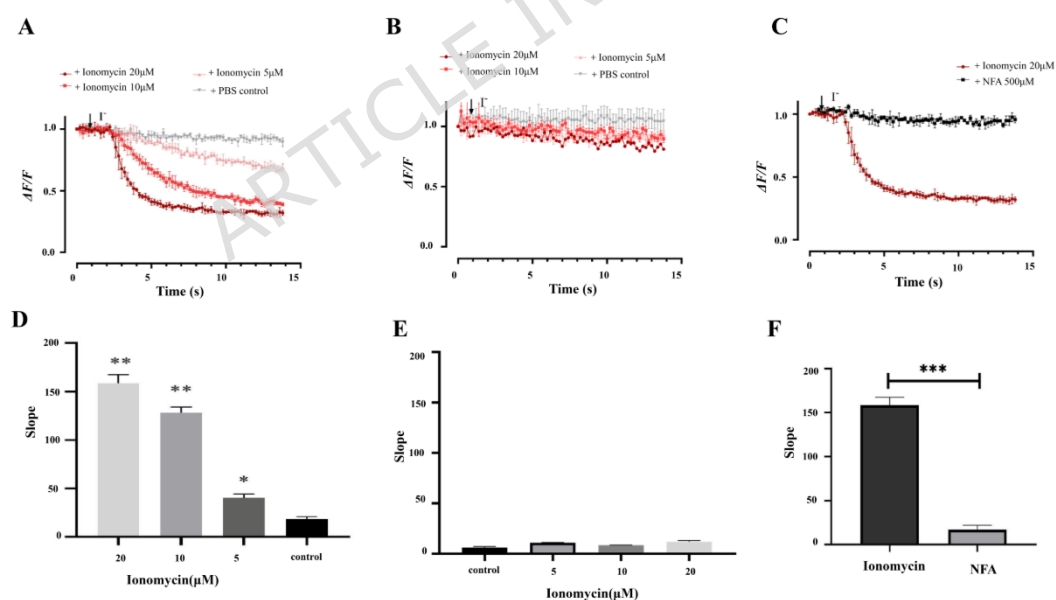


Figure 6: Validation of the Functionality of the High-Throughput Screening Cell Model for ANO1 Modulators Using Fluorescence Quenching Kinetics Experiments. A: ANO1-expressing cells treated with different concentrations of Ionomycin;

B: Parental FRT cells treated with different concentrations of ionomycin; C: ANO1 activation by 20 μ M Ionomycin followed by NFA (500 μ M) inhibition; D: Slope values of the fluorescence quenching curves in group A ($*P < 0.05$, $**P < 0.01$); E: Slope values of the fluorescence quenching curves in group B (ns, no significant difference); F: Slope values of the fluorescence quenching curves in group C ($***P < 0.001$).

3.4. Z'-Factor Assessment of ANO1 High-Throughput Screening Cell Model Stability

The Z' factor evaluation results showed a significant difference between the experimental group and the negative control group ($P < 0.001$). The values were $SD_{\text{positive}} = 6.12$, $SD_{\text{BACK}} = 3.10$, $M_{\text{positive}} = 108.37$, and $M_{\text{BACK}} = 21.67$. Using the Z' factor formula $Z' = 1 - 3 \times (SD_{\text{positive}} + SD_{\text{BACK}}) / (M_{\text{positive}} - M_{\text{BACK}})$, the Z' factor was calculated to be 0.69. This indicates that the high-throughput screening cell model for ANO1 modulators constructed in this experiment has good stability (see Figure 7).

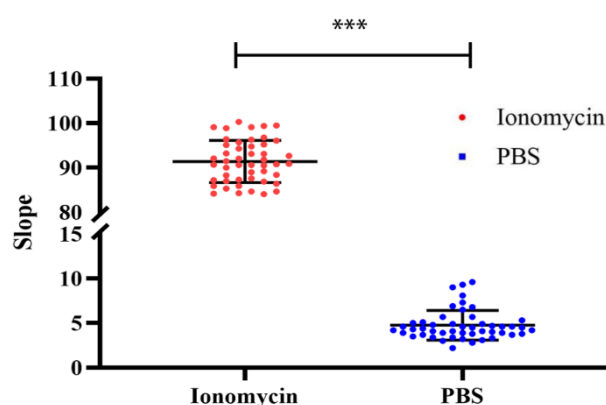


Figure 7: Evaluation of the Z' Factor for the High-Throughput Screening Cell Model for ANO1 Modulators ($***P < 0.001$).

3.5. Concentration- and Time-Dependent Activation of ANO1 by Eact

Patch-clamp experiments have confirmed that ANO1 channels exhibit typical current rundown under sustained stimulation with high concentrations of Ca^{2+} . However, whether this time-dependent decline also occurs during prolonged exposure to indirect activators such as Eact remains unclear. This issue is particularly critical for the screening of ANO1 activators—if rundown causes a reduction in current over time, potent candidates may be misjudged or overlooked. To address this, we utilized the established high-throughput screening model for CaCCs modulators to systematically assess whether ANO1 channel responses change over the course of Eact exposure, and whether channel activation decreases or is completely lost with time.

3.5.1. Dose-response curve for Eact, an indirect activator of ANO1

Fluorescence quenching kinetics revealed that the extent of signal reduction increased progressively with rising concentrations of Eact (Figure 8A). Further analysis of the initial slope values of the quenching curves at different concentrations showed that the slope increased with agonist concentration, demonstrating a clear dose-

dependent relationship (Figure 8B). The fitted dose-response curve indicated that the half-maximal effective concentration (EC_{50}) of Eact was $7.485 \mu\text{M}$. Concentrations ranging from 20 to $100 \mu\text{M}$ were defined as the high-dose range, while those below $20 \mu\text{M}$ exhibited a significant dose-dependent relationship with ANO1 channel activation (Figure 8C).

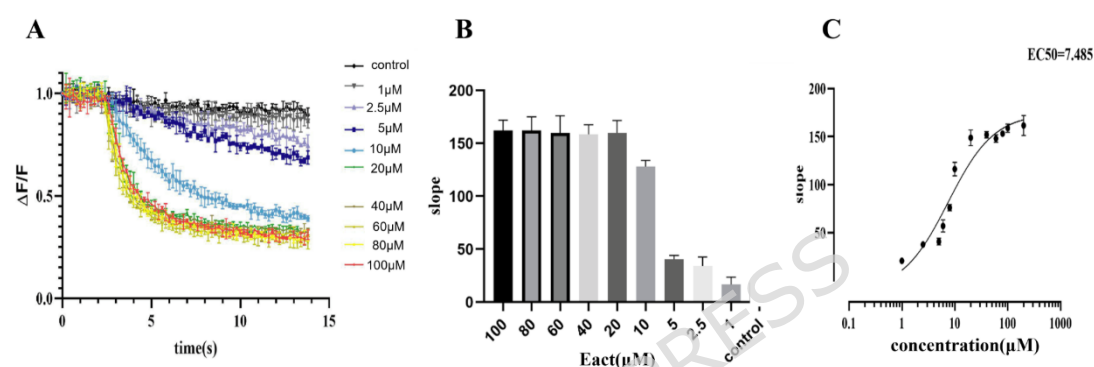


Figure 8: Fluorescence Quenching Kinetics Experiments for the ANO1 Agonist Eact. A: Fluorescence quenching curves at different concentrations of Eact. Each data point represents the difference between the relative fluorescence intensity value of each individual point and the first recorded value of the experiment (ΔF) divided by the first recorded value (F); B: Slope values of the fluorescence quenching curves at different concentrations of Eact; C: Dose-response curve of the slope values of the fluorescence quenching curves with Eact concentration.

3.5.2. Effect of Eact on the Sustained Activation of ANO1 Channels

Based on the dose-response relationship of Eact, this study further evaluated the effect of agonist concentration on the sustained activation of the ANO1 channel. Fluorescence quenching kinetics showed that under low Eact concentrations, channel activity increased with concentration and remained relatively stable over a 40-minute period (Figure 9A). In contrast, at high concentrations, channels were initially fully activated but exhibited a marked decline in activity after approximately 20 minutes, with some conditions approaching a closed state (Figure 9B). These findings demonstrate that agonist concentration has a significant impact on channel activity and should be carefully considered in the design of future screening strategies.

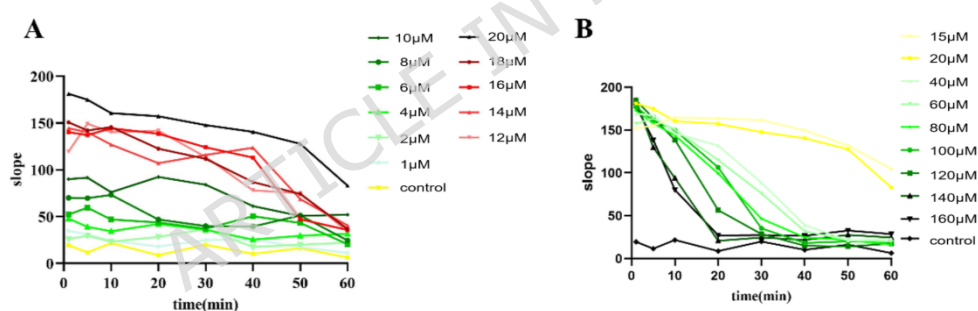


Figure 9: Fluorescence quenching kinetics experiments investigating the time-dependent changes in ANO1 channel opening with low concentration agonists (A) and high concentration agonists (B).

3.6. Optimization of the Screening Strategy for the High-Throughput Screening Cell Model of ANO1 Modulators

3.6.1. Optimizing the Screening Strategy for ANO1 Agonists Based on the Effect of Agonist Concentration on ANO1 Channel Opening Time

This study found that under conditions of sustained activation by high calcium concentrations or high concentrations of agonists, the ANO1 channel exhibited a pronounced time-dependent current rundown. This feature reveals a potential limitation in conventional high-throughput screening strategies for ANO1 modulators using the YFP iodide quenching method. Specifically, under standard screening conditions, the compound concentration is typically set at around 200 μM , with each well on a 96-well plate requiring approximately 15 seconds for detection. As a result, the total time to complete one screening unit exceeds 30 minutes. During this period, wells positioned later in the sequence may be affected by rundown, resulting in decreased or closed channel activity and an inability to detect fluorescence quenching signals—leading to missed identification of potentially high-efficacy agonists (Figure 10A).

To reduce the risk of false negatives and improve screening accuracy, this study proposes the following strategy optimizations: First, a column-wise serial dilution scheme can be applied across the

96-well plate, enabling 12 candidate compounds to be screened per plate. If a positive signal is observed in any column, the corresponding compound can be individually validated using patch-clamp experiments, effectively balancing screening throughput and hit accuracy. Second, the total detection time can be appropriately shortened. Our experimental results confirm that under high agonist concentrations, ANO1 channel activation can be stably maintained for 10–15 minutes. Therefore, reducing the number of wells per plate can shorten the total screening time, ensuring that key activation signals are captured before channel rundown occurs (Figure 10B).

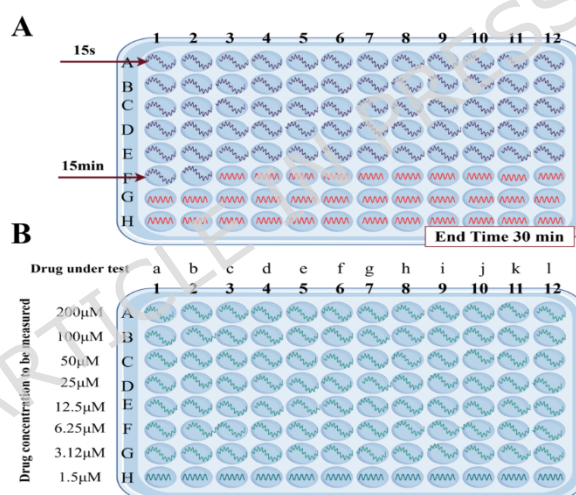


Figure 10: Schematic Diagrams Showing the Flaws (A) and Optimized Strategy (B) for Screening ANO1 Agonists Using the YFP Iodide Quenching Method (by Fig Draw).

3.6.2. Optimization of ANO1 Inhibitor Screening Strategy

To address the limitations associated with traditional ANO1 inhibitor screening, we proposed an optimized strategy based on the electrophysiological properties of the channel. In the conventional approach, test compounds are typically pre-incubated with cells, followed by the addition of ATP as an indirect ANO1 activator to elevate intracellular calcium levels. However, many small molecules may interfere with upstream calcium signaling pathways rather than directly targeting ANO1, leading to a high rate of false positives and increasing the validation burden in subsequent patch-clamp experiments (see schematic diagram 11A).

In the revised strategy, an appropriate concentration of an ANO1 agonist is first applied to ensure sustained channel activation throughout the screening period. Test compounds are then added and allowed to act under this activated state. Compounds that do not directly inhibit ANO1 are unlikely to affect the open channel conformation, thereby enabling the specific identification of direct ANO1 inhibitors (see schematic diagram 11B). This approach minimizes off-target interference from calcium signaling modulators and improves both screening specificity and downstream efficiency.

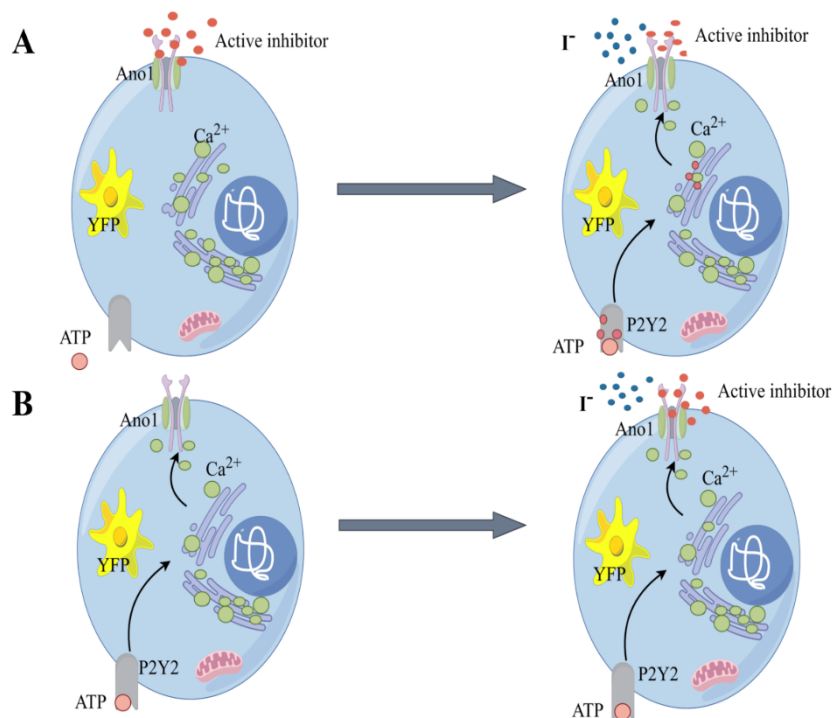


Figure 11: Schematic Diagrams Showing the Flaws (A) and Optimized Strategy (B) for Screening ANO1 Inhibitors Using the YFP Iodide Quenching Method (by Fig Draw).

4. Discussion

This study focuses on the functional characteristics of the calcium-activated chloride channel family member ANO1 and the key challenges associated with its application in HTS platforms. The goal is to establish a more specific and reliable screening strategy for the development of small-molecule modulators targeting CaCCs. ANO1 is widely expressed in the airways^[24], gastrointestinal tract^[25], glands^[26], sensory neurons^[1], and various tumor tissues^[27]. It not only participates in ion transport, secretion regulation, and smooth

muscle contraction^[28], but also plays crucial roles in tumor cell proliferation, migration, and modulation of the tumor microenvironment^[29, 30]. Thus, ANO1 has emerged as a potential therapeutic target for multiple diseases, including CF (Cystic fibrosis, CF)^[31], asthma^[32], pain^[33], and colorectal cancer^[34]. However, the number of ANO1 agonists currently available for basic or clinical research is extremely limited, and most lack target selectivity^[35]. For instance, INS37217 and MOLI1901, though advanced into clinical studies for CF, do not selectively activate ANO1 and are associated with broad off-target effects, which may lead to adverse outcomes^[36]. This significantly restricts their clinical translation and highlights the limitations of current screening methods in identifying highly selective modulators. Therefore, establishing a screening model with both functional sensitivity and signal stability, along with an optimized screening protocol, is essential for advancing efficient CaCCs-targeted drug development.

Although ANO1 and ANO2 have been confirmed as representative CaCCs within the anoctamin family, the channel properties, tissue distribution, and physiological functions of other family members remain unclear. Heterologous expression systems are commonly used for functional studies; however, some isoforms fail to localize to the plasma membrane after transfection, suggesting that their

channel activity may depend on auxiliary subunits or that they may not function as membrane channels at all. Among these members, ANO7 has been particularly controversial. Moreover, some researchers have questioned whether ANO7 is a membrane protein at all, as there is currently no definitive evidence confirming its identity as a functional membrane channel^[37]. Previous studies have shown that among the ten members of the anoctamin family (ANO1-ANO10)^[38], ANO1, ANO6, ANO7, ANO8, ANO9, and ANO10 are predominantly expressed in epithelial tissues, while ANO2, ANO3, ANO4, and ANO5 are commonly expressed in neurons and muscle tissues. Among them, ANO1, ANO2, ANO6, and ANO7 have been confirmed to mediate Ca²⁺-activated Cl⁻ currents, although they exhibit significant differences in calcium sensitivity and activation kinetics. Therefore, further electrophysiological studies are essential to clarify the functional classification of these channels^[39].

In terms of screening libraries, current efforts are primarily focused on small-molecule compounds, with typical library sizes around 10⁵. These compounds are mainly derived from natural products and synthetic chemical libraries. Natural products tend to exhibit higher bioactivity but are often difficult to extract and purify, while synthetic compounds have defined structures but relatively lower activity and higher production costs. Structural optimization

and modification based on bioactive scaffolds from natural products represent a promising and cost-effective strategy to enhance screening efficiency and obtain higher-potency candidates.

In compound screening, current efforts are primarily focused on small-molecule compounds, with typical library sizes around 10^5 to balance chemical diversity and high-throughput efficiency^[40]. These compounds are mainly derived from natural products or synthetic chemical libraries. Natural products are characterized by high structural complexity and notable bioactivity, and have long been considered valuable resources in drug discovery. However, their extraction and purification processes are often technically challenging and time-consuming^[41]. In contrast, synthetic small molecules offer well-defined structures and controllable synthetic routes, but generally exhibit lower biological relevance and are costly to construct on a large scale^[42]. As a result, structural optimization and semi-synthetic modification of bioactive natural scaffolds have emerged as a practical strategy to enhance compound activity while maintaining screening efficiency.

In this study, we constructed a stable, ANO1-expressing HTS cell model based on the YFP-H148Q/I152L fluorescence quenching mechanism. Evaluation using the Z' factor confirmed that the cell model has a high signal-to-noise ratio, stability, and strong

applicability in multi-well plate screening assays. However, during our experiments, we observed a significant current rundown phenomenon in ANO1 channels under sustained stimulation with high concentrations of Ca^{2+} or agonists. This time-dependent decrease in channel activity could potentially result in the missed detection of highly effective small-molecule agonists prone to inducing rundown, particularly when higher concentrations of compounds (200 μM) or longer screening durations (>30 min) are employed. Additionally, the current YFP iodide fluorescence quenching-based approach for screening CaCCs modulators faces several limitations^[43, 44]. Firstly, there is an issue with insufficient duration of agonist effects, leading to possible missed detections. Secondly, during inhibitor screening, compounds may non-specifically target other calcium-release pathways, resulting in false-positive outcomes.

To address this issue, the screening strategy was systematically optimized in this study. On one hand, a serial dilution approach was applied to the small-molecule compounds to reduce the risk of channel activity suppression caused by high drug concentrations. On the other hand, the number of detection wells per screening unit was reduced to significantly shorten the overall detection duration, ensuring that signal acquisition occurs while channel activity remains high. In addition, during inhibitor screening, a sequential protocol of

"activating the channel first, then adding candidate compounds" was introduced to avoid interference from non-specific small molecules acting on upstream calcium signaling pathways, thereby enabling more accurate identification of modulators that directly target ANO1.

To further determine whether the rundown phenomenon is a general feature among members of the Anoctamin family of CaCCs, this study selected ANO2—the isoform most homologous to ANO1—as a comparative model. Under inside-out patch-clamp recording conditions, ANO2 displayed stable current responses at the same calcium concentrations, without showing significant rundown, in contrast to the pronounced decline observed in ANO1. This difference may be attributed to ANO2's lower calcium sensitivity relative to ANO1. Previous studies have confirmed this lower sensitivity by comparing EC₅₀ values^[45]. Notably, while some previous studies^[46-48] have suggested that certain splice variants of ANO2 may exhibit rundown-like behavior or slight inactivation under specific conditions—such as calmodulin (CaM)-mediated regulation these phenomena are typically limited to specific isoforms or mechanisms, and differ from the sustained activation stability observed under our standardized conditions. Our findings further support that ANO2 possesses a greater ability to maintain current in high-Ca²⁺ environments compared to ANO1, highlighting its overall electrophysiological stability under calcium signaling conditions.

From the perspective of screening platform development,

although ANO2 may be considered a favorable channel model due to its superior current stability, ANO1 was ultimately selected to construct the YFP-H148Q/I152L fusion protein cell model. This decision was supported by ANO1's well-characterized roles in multiple disease models, along with its greater calcium sensitivity and signal responsiveness. As such, an ANO2-YFP-H148Q/I152L cell line was not established in this study.

Nevertheless, we acknowledge that a screening system relying solely on ANO1 may present limitations in identifying isoform-selective modulators. To comprehensively assess the specificity and selectivity of novel compounds, future studies should explore the development of comparative models incorporating additional ANO family members, including ANO2, thereby improving the resolution and broader applicability of the screening platform.

During the validation of the stable cell lines, RT-PCR, fluorescence imaging, and flow cytometry confirmed the expression and subcellular localization of ANO1, ANO2, and YFP-H148Q/I152L; however, these approaches do not allow quantitative assessment of the actual abundance of channel proteins at the plasma membrane. Given that membrane expression levels of ion channels can markedly influence current amplitude, open probability, and Ca^{2+} sensitivity, differences in expression among stable cell lines may affect the

performance of downstream functional assays and compound selectivity analyses^[49, 50].

In this study, FRT cells were selected as the parental cell line based on their well-established use in chloride channel high-throughput screening and their low background activity. FRT cells form stable and compact epithelial monolayers, which facilitates uniform exposure to extracellular I^- and enables consistent and reproducible YFP-H148Q/I152L fluorescence-quenching kinetics. More importantly, FRT cells do not express endogenous ANO1 and lack detectable Ca^{2+} -activated Cl^- currents^[38], providing a near “background-free” system for functional analysis of exogenously expressed Anoctamin channels.

The functional results obtained in this study—including fluorescence quenching kinetics and patch-clamp recordings—demonstrate that the current expression levels are sufficient to support stable operation of the screening platform. Future work will incorporate quantitative expression analyses together with high-resolution electrophysiological and imaging approaches to further improve the accuracy and robustness of the screening system.

In addition, although this study achieved meaningful improvements in screening strategy optimization, several limitations remain. First, while the gradient dilution strategy enhanced the

detection rate of positive signals, it concurrently reduced the screening throughput per batch. Second, this study primarily focused on two well-characterized members of the Anoctamin family, ANO1 and ANO2. Other isoforms with more controversial or less-defined functional roles, such as ANO6 and ANO7, were not systematically investigated. Future research should aim to expand this analysis to provide a more comprehensive understanding of the functional and pharmacological diversity across the Anoctamin family.

5. Conclusion

This study proposes and validates a HTS strategy that integrates ANO1 electrophysiological characteristics with dynamic functional responses, significantly enhancing the specificity and accuracy of ANO1 modulator identification. By simultaneously addressing channel activity sensitivity and platform adaptability, this strategy lays a foundation for the future discovery of potent and selective CaCCs modulators.

Author Contributions: Y.W. and K.Z. conceived of and designed the research. L.Y., L.L., H.H., S.C. and Z.Q. performed the experiments. K.Q., W.Z. and F.H. interpreted the results of the experiments. Y.W. and K.Z. drafted the manuscript and edited and revised the manuscript. All authors read and approved the final.

Funding: This work was partly supported by the Project of Jilin Provincial Department of Education (JJKH20220462KJ, JJKH20220473SK and JJKH20240596KJ), the Project of Science and Technology Department of Jilin Province (YDZJ202401007ZYTS), Jilin Medical College graduate innovation program (2023zyc04), "Meikang Shengde" student scientific research and innovation project of Inspection College of Jilin Medical University(2023jymkz002) , Jilin University of Medicine 2024 College Student Innovation and Entrepreneurship Training Program (S202413706007) , Jilin Province Health and Health Technology Capacity Enhancement Project (2024A094) , National Natural Science Foundation of China(81173109).

Institutional Review Board Statement: Not applicable.

Informed Consent Statement: Not applicable.

Data Availability Statement: Raw data and images can be obtained from the corresponding authors.

Acknowledgments: Y.W., K.Z., K.Q., W.Z. and F.H. contributed equally to this work, and they are responsible for the idea, funding, and paper editing.

Conflicts of Interest: The authors declare no conflict of interest.

Sample Availability: Samples of the compounds are not available from the authors.

References

- [1] YANG Y D, CHO H, KOO J Y, et al. TMEM16A confers receptor-activated calcium-dependent chloride conductance [J]. *Nature*, 2008, 455(7217): 1210-5.
- [2] CAPUTO A, CACI E, FERRERA L, et al. TMEM16A, a membrane protein associated with calcium-dependent chloride channel activity [J]. *Science (New York, NY)*, 2008, 322(5901): 590-4.
- [3] SCHROEDER B C, CHENG T, JAN Y N, et al. Expression cloning of TMEM16A as a calcium-activated chloride channel subunit [J]. *Cell*, 2008, 134(6): 1019-29.
- [4] MANSOURA M K, BIWERSI J, ASHLOCK M A, et al. Fluorescent chloride indicators to assess the efficacy of CFTR cDNA delivery [J]. *Human gene therapy*, 1999, 10(6): 861-75.
- [5] SCUDIARI P, SONDO E, CACI E, et al. TMEM16A-TMEM16B chimaeras to investigate the structure-function relationship of calcium-activated chloride channels [J]. *The Biochemical journal*, 2013, 452(3): 443-55.
- [6] RHODEN K J, CIANCHETTA S, STIVANI V, et al. Cell-based imaging of sodium iodide symporter activity with the yellow fluorescent protein variant YFP-H148Q/I152L [J]. *American journal of physiology Cell physiology*, 2007, 292(2): C814-23.
- [7] SEO Y, LEE H K, PARK J, et al. Ani9, A Novel Potent Small-Molecule ANO1 Inhibitor with Negligible Effect on ANO2 [J]. *PloS one*, 2016, 11(5): e0155771.
- [8] OH S J, HWANG S J, JUNG J, et al. MONNA, a potent and selective blocker for transmembrane protein with unknown function 16/anoctamin-1 [J]. *Molecular pharmacology*, 2013, 84(5): 726-35.
- [9] LIU Y, ZHANG H, MEN H, et al. Volume-regulated Cl(-) current: contributions of distinct Cl(-) channels and localized Ca(2+) signals [J]. *Am J Physiol Cell Physiol*, 2019, 317(3): C466-c80.
- [10] ZHENG K, XU H J, ZANG Y X, et al. [Effect of enhanced green fluorescent protein fusion on Ano1 physiological feature] [J]. *Sheng Li Xue Bao*, 2015, 67(6): 623-8.
- [11] CABRITA I, BENEDETTO R, FONSECA A, et al. Differential effects of anoctamins on intracellular calcium signals [J]. *FASEB journal : official publication of the Federation of American Societies for Experimental Biology*, 2017, 31(5): 2123-34.
- [12] NAMKUNG W, PHUAN P W, VERKMAN A S. TMEM16A inhibitors reveal TMEM16A as a minor component of calcium-activated chloride channel conductance in airway and intestinal epithelial cells [J]. *The Journal of biological chemistry*, 2011, 286(3): 2365-74.

- [13] OBERGRUSSBERGER A, FRIIS S, BRÜGGEMANN A, et al. Automated patch clamp in drug discovery: major breakthroughs and innovation in the last decade [J]. *Expert Opin Drug Discov*, 2021, 16(1): 1-5.
- [14] VERHOECKX K, COTTER P, LÓPEZ-EXPÓSITO I, et al. The Impact of Food Bioactives on Health: in vitro and ex vivo models. Cham (CH); Springer Copyright 2015, The Editor(s) (if applicable) and the Author(s). 2015.
- [15] BRITSCHGI A, BILL A, BRINKHAUS H, et al. Calcium-activated chloride channel ANO1 promotes breast cancer progression by activating EGFR and CAMK signaling [J]. *Proceedings of the National Academy of Sciences of the United States of America*, 2013, 110(11): E1026-34.
- [16] LI Y, ZHANG J, HONG S. ANO1 as a marker of oral squamous cell carcinoma and silencing ANO1 suppresses migration of human SCC-25 cells [J]. *Medicina oral, patologia oral y cirugía bucal*, 2014, 19(4): e313-9.
- [17] SEO Y, PARK J, KIM M, et al. Inhibition of ANO1/TMEM16A Chloride Channel by Idebenone and Its Cytotoxicity to Cancer Cell Lines [J]. *PloS one*, 2015, 10(7): e0133656.
- [18] TAYLOR R D, JEWSBURY P J, ESSEX J W. A review of protein-small molecule docking methods [J]. *Journal of computer-aided molecular design*, 2002, 16(3): 151-66.
- [19] HAGA J H, ICHIKAWA K, DATE S. Virtual Screening Techniques and Current Computational Infrastructures [J]. *Current pharmaceutical design*, 2016, 22(23): 3576-84.
- [20] LEE Y H, YI G S. Prediction of Novel Anoctamin1 (ANO1) Inhibitors Using 3D-QSAR Pharmacophore Modeling and Molecular Docking [J]. *International journal of molecular sciences*, 2018, 19(10).
- [21] CHOI S H, RYU S, SIM K, et al. Anti-glioma effects of 2-aminothiophene-3-carboxamide derivatives, ANO1 channel blockers [J]. *European journal of medicinal chemistry*, 2020, 208: 112688.
- [22] PAULINO C, NELDNER Y, LAM A K, et al. Structural basis for anion conduction in the calcium-activated chloride channel TMEM16A [J]. *eLife*, 2017, 6.
- [23] DANG S, FENG S, TIEN J, et al. Cryo-EM structures of the TMEM16A calcium-activated chloride channel [J]. *Nature*, 2017, 552(7685): 426-9.
- [24] OUSINGSAWAT J, CENTEIO R, REYNE N, et al. Inhibition of mucus secretion by niclosamide and benzbromarone in airways and intestine [J]. *Scientific reports*, 2024, 14(1): 1464.
- [25] STREGÉ P R, GIBBONS S J, MAZZONE A, et al. EAVK segment "c" sequence confers Ca(2+)-dependent changes to the kinetics of full-length human Ano1 [J]. *American journal of physiology Gastrointestinal and liver physiology*, 2017, 312(6): G572-g9.
- [26] SHIN Y, LEE S W, NAMKOONG E, et al. Epigenetic Modification as a Regulatory Mechanism for Spatiotemporal Dynamics of ANO1 Expression in Salivary Glands [J]. *International journal of molecular sciences*, 2019, 20(24).

- [27] DUVVURI U, SHIWARSKI D J, XIAO D, et al. TMEM16A induces MAPK and contributes directly to tumorigenesis and cancer progression [J]. *Cancer research*, 2012, 72(13): 3270-81.
- [28] PEDEMONTE N, GALIETTA L J. Structure and function of TMEM16 proteins (anoctamins) [J]. *Physiological reviews*, 2014, 94(2): 419-59.
- [29] QU Z, YAO W, YAO R, et al. The Ca²⁺-activated Cl⁻ channel, ANO1 (TMEM16A), is a double-edged sword in cell proliferation and tumorigenesis [J]. *Cancer medicine*, 2014, 3(3): 453-61.
- [30] RUIZ C, MARTINS J R, RUDIN F, et al. Enhanced expression of ANO1 in head and neck squamous cell carcinoma causes cell migration and correlates with poor prognosis [J]. *PloS one*, 2012, 7(8): e43265.
- [31] PINTO M C, BOTELHO H M, SILVA I A L, et al. Systems Approaches to Unravel Molecular Function: High-content siRNA Screen Identifies TMEM16A Traffic Regulators as Potential Drug Targets for Cystic Fibrosis [J]. *Journal of molecular biology*, 2022, 434(5): 167436.
- [32] WU A, KUFORJI A, ZHANG Y, et al. TMEM16A Antagonism: Therapeutic Potential with Desensitization of β -Agonist Responsiveness in Asthma [J]. *American journal of respiratory cell and molecular biology*, 2025, 72(5): 510-9.
- [33] CAO X, ZHOU Z, TIAN Y, et al. Opposing roles of E3 ligases TRIM23 and TRIM21 in regulation of ion channel ANO1 protein levels [J]. *The Journal of biological chemistry*, 2021, 296: 100738.
- [34] JIANG Y, CAI Y, SHAO W, et al. MicroRNA-144 suppresses aggressive phenotypes of tumor cells by targeting ANO1 in colorectal cancer [J]. *Oncology reports*, 2019, 41(4): 2361-70.
- [35] MITRI C, SHARMA H, CORVOL H, et al. TMEM16A/ANO1: Current Strategies and Novel Drug Approaches for Cystic Fibrosis [J]. *Cells*, 2021, 10(11).
- [36] SEO Y, ANH N H, HEO Y, et al. Novel ANO1 Inhibitor from *Mallotus apelta* Extract Exerts Anticancer Activity through Downregulation of ANO1 [J]. *International journal of molecular sciences*, 2020, 21(18).
- [37] DURAN C, QU Z, OSUNKOYA A O, et al. ANOs 3-7 in the anoctamin/Tmem16 Cl⁻ channel family are intracellular proteins [J]. *American journal of physiology Cell physiology*, 2012, 302(3): C482-93.
- [38] SCHREIBER R, ULIYAKINA I, KONGSUPHOL P, et al. Expression and function of epithelial anoctamins [J]. *J Biol Chem*, 2010, 285(10): 7838-45.
- [39] TIAN Y, SCHREIBER R, KUNZELMANN K. Anoctamins are a family of Ca²⁺-activated Cl⁻ channels [J]. *Journal of cell science*, 2012, 125(Pt 21): 4991-8.
- [40] MACARRON R, BANKS M N, BOJANIC D, et al. Impact of high-throughput screening in biomedical research [J]. *Nature reviews Drug discovery*, 2011, 10(3): 188-95.
- [41] NEWMAN D J, CRAGG G M. Natural Products as Sources of New Drugs over the Nearly Four Decades from 01/1981 to 09/2019 [J]. *Journal of natural products*, 2020, 83(3): 770-803.
- [42] LI J W, VEDERAS J C. Drug discovery and natural products: end of an era or an endless frontier? [J]. *Science (New York, NY)*, 2009, 325(5937): 161-5.

- [43]NAMKUNG W, THIAGARAJAH J R, PHUAN P W, et al. Inhibition of Ca²⁺-activated Cl⁻ channels by gallotannins as a possible molecular basis for health benefits of red wine and green tea [J]. *FASEB journal : official publication of the Federation of American Societies for Experimental Biology*, 2010, 24(11): 4178-86.
- [44]SEO Y, KIM J, CHANG J, et al. Synthesis and biological evaluation of novel Ani9 derivatives as potent and selective ANO1 inhibitors [J]. *European journal of medicinal chemistry*, 2018, 160: 245-55.
- [45]LEE J, JUNG J, TAK M H, et al. Two helices in the third intracellular loop determine anoctamin 1 (TMEM16A) activation by calcium [J]. *Pflugers Archiv : European journal of physiology*, 2015, 467(8): 1677-87.
- [46]YANG T, HENDRICKSON W A, COLECRAFT H M. Preassociated apocalmodulin mediates Ca²⁺-dependent sensitization of activation and inactivation of TMEM16A/16B Ca²⁺-gated Cl⁻ channels [J]. *Proceedings of the National Academy of Sciences of the United States of America*, 2014, 111(51): 18213-8.
- [47]PONISSERTY SAIDU S, STEPHAN A B, TALAGA A K, et al. Channel properties of the splicing isoforms of the olfactory calcium-activated chloride channel Anoctamin 2 [J]. *The Journal of general physiology*, 2013, 141(6): 691-703.
- [48]PIFFERI S, DIBATTISTA M, MENINI A. TMEM16B induces chloride currents activated by calcium in mammalian cells [J]. *Pflugers Archiv : European journal of physiology*, 2009, 458(6): 1023-38.
- [49]ALVAREZ O, GONZALEZ C, LATORRE R. Counting channels: a tutorial guide on ion channel fluctuation analysis [J]. *Adv Physiol Educ*, 2002, 26(1-4): 327-41.
- [50]NIRENBERG V A, YIFRACH O. Bridging the Molecular-Cellular Gap in Understanding Ion Channel Clustering [J]. *Front Pharmacol*, 2019, 10: 1644.